SUPPLEMENTAL DATA

SUPPLEMENTAL FIGURES AND LEGENDS

Figure S1 (related to Fig. 1)

A Young and aged samples

Sample Code	Gender	Age
Young-2130§	M	27
Young-4018^*	M	26
Young-4040^	M	24
Young-4066^*	M	28
Young-4188^	M	19
Young-4215^	F	27
Young-4218^	M	28
Young-4259^	M	27
Young-4279^	M	27
Young-4532§	M	26
Young-4698§	F	33
Young-4742§	F	27
Aged-368^§	F	61
Aged-380^*	F	65
Aged-401^§	F	64
Aged-402^*	F	82
Aged-410^§	M	66
Aged-415^	F	66
Aged-416^	M	62
Aged-426^	F	61
Aged-439§	F	N/A (>60)
Aged-457§*	F	77
Aged-620§*	M	68
Aged-654§*	F	61

B GSEA in HSC aging

NAME	SIZE	NES	NOM p-val	FDR q val
KEGG_OXIDATIVE_PHOSPHORYLATION	106	-2.18	<0.001	<0.001
KEGG_HUNTINGTONS_DISEASE	161	-2.08	<0.001	0.002
KEGG_RIBOSOME	86	-1.96	<0.001	0.006
KEGG_DNA_REPLICATION	36	-1.94	0.002	0.007
KEGG_PROTEASOME	43	-1.9	<0.001	0.009

C GSEA in HPC aging

NAME	SIZE	NES	NOM p-val	FDR q val
KEGG_SYSTEMIC_LUPUS_ERYTHEMATOSUS	132	2.978	<0.001	<0.001
KEGG_MISMATCH_REPAIR	23	-2.14	<0.001	<0.001
KEGG_HOMOLOGOUS_RECOMBINATION	28	-2.1	<0.001	<0.001
KEGG_GLYCOSAMINOGLYCAN_BIOSYNTHESIS_HEPARAN_SULFATE	26	-2.01	<0.001	0.001
KEGG_AMINOACYL_TRNA_BIOSYNTHESIS	41	-1.87	<0.001	0.009

D Gene signature of human HSC aging

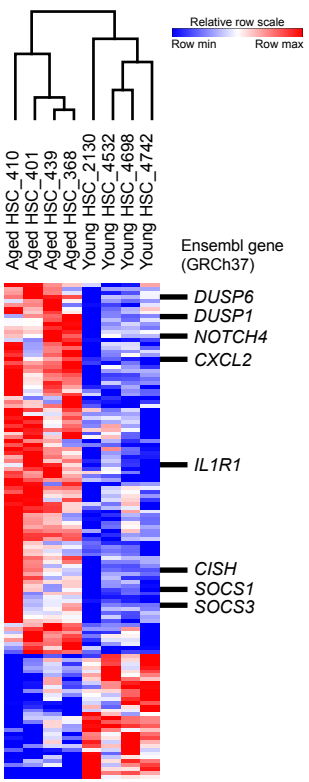

E Gene signature of human HPC aging

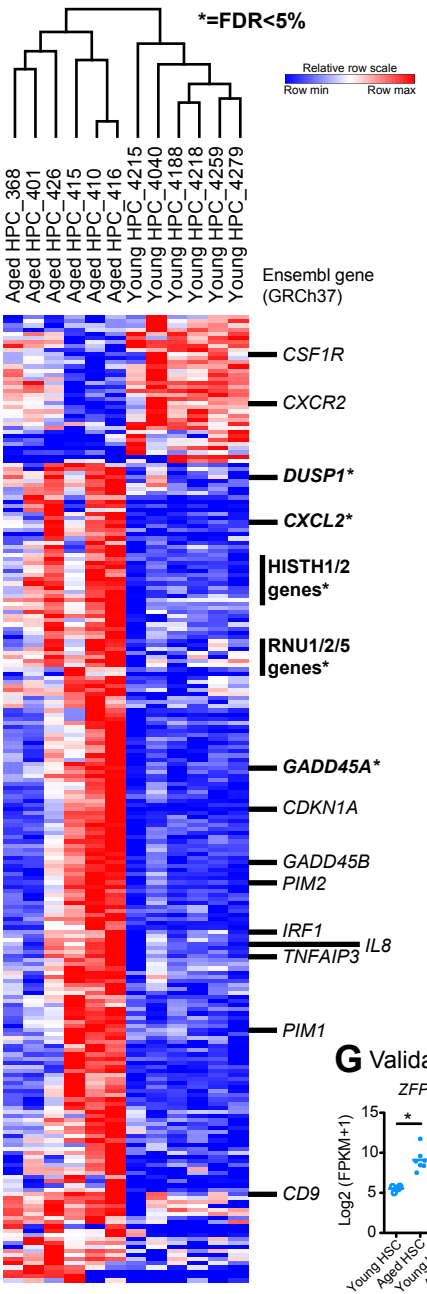

F Splice isoform signature of human HPC aging v. cord blood

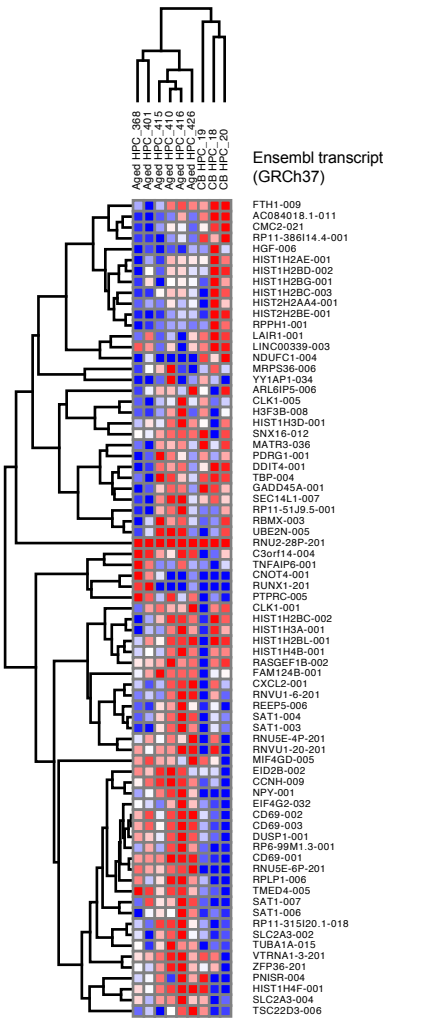

G Validation of common isoforms in HSC and HPC

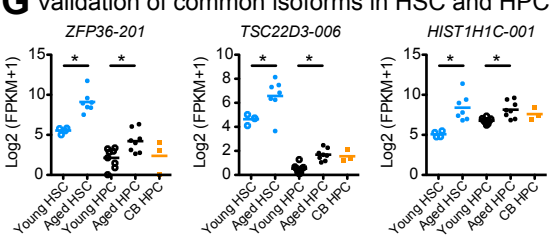

Figure S1. Primary Samples, Gene Set Enrichment Analyses and Whole Gene Expression Signatures of Human HSC and HPC Aging.

(A) Primary patient bone marrow samples used in RNA-sequencing studies of normal HSC and HPC. ^Used in HPC RNA-Seq, §Used in HSC RNA-Seq, *Validation cohorts, N/A = not available.

(B, C) For FACS-purified hematopoietic stem ($CD34^+CD38^-$ Lin^-, n=4 per group) and progenitor ($CD34^+CD38^+$ Lin^-, n=6 per group) cells from normal young and aged BM samples, gene and isoform expression data in FPKM was obtained from RNA-Seq datasets (see Experimental Procedures and Supplemental Experimental Procedures for details). Gene set enrichment analyses (GSEA) were performed to identify significant KEGG pathways. Top gene sets deregulated in aged versus young normal HSC (B) and HPC (C) are shown (false discovery rate, FDR<1%). NES=normalized enrichment score.

(D, E) Log 2 fold change (L2FC) and *p* values were computed from gene expression data (FPKM+1, aged/young). Profiles of all differentially expressed genes ($p<0.05$) in human HSC (D) and HPC (E) aging (absolute L2FC>1) are shown.

(F) Comparison of HPC aging isoform signature with transcript expression levels in cord blood (CB) progenitors (n=3) (Jiang et al., 2013).

(G) Validation across all sequenced patient samples showing relative expression levels (log2 FPKM+1) of abundant transcripts that were commonly differentially expressed in young versus aged HSC and HPC in the discovery sample sets. For this analysis, three additional HSC samples were included (run on NextSeq platform as compared to HiSeq platform used in discovery sets), and four additional HPC samples were used for validation (*$p<0.05$).

Figure S2 (related to Fig. 2)

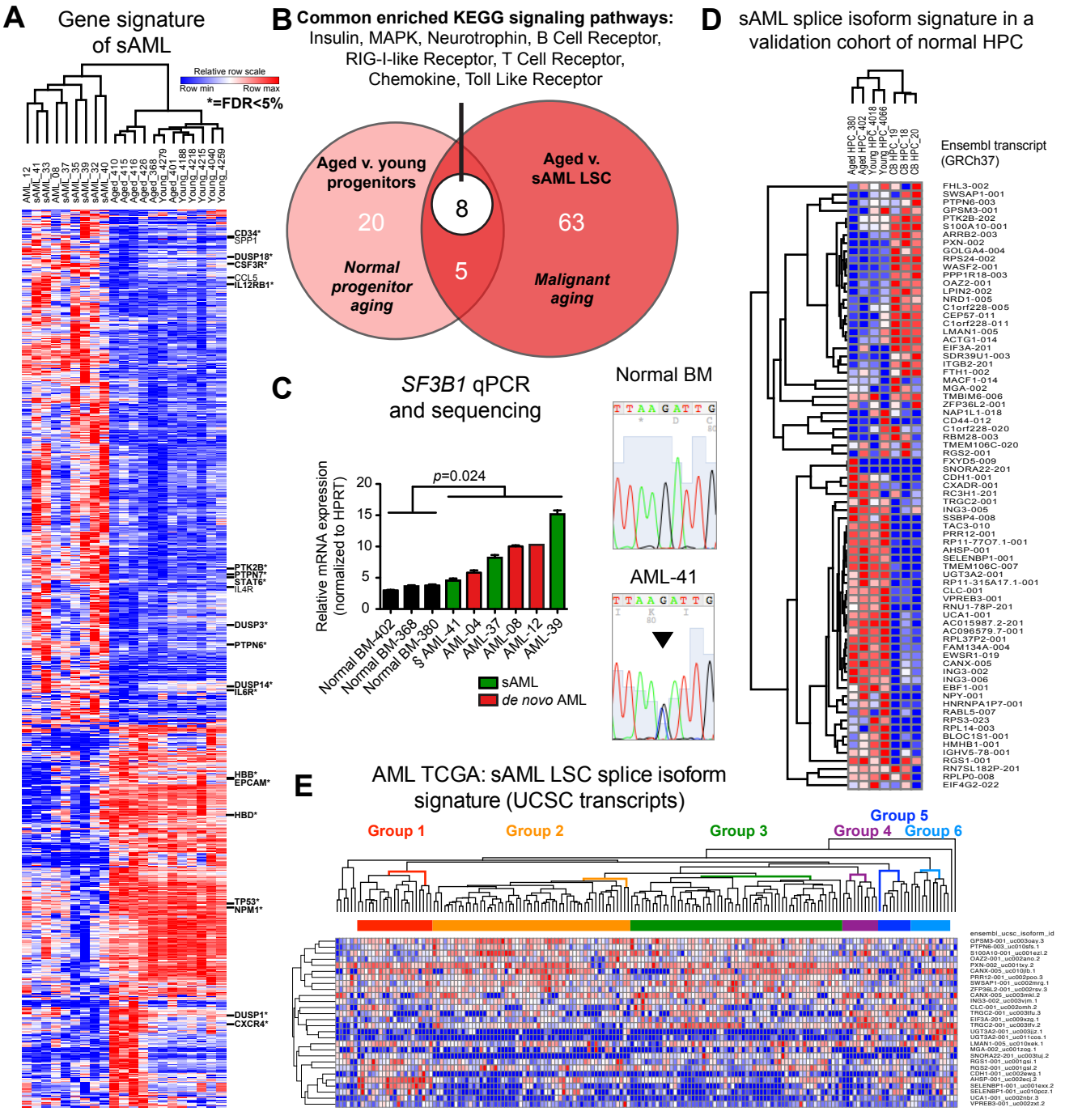

Figure S2. Whole Gene Expression Signatures of sAML LSC. For FACS-purified sAML and normal progenitor ($CD34^+CD38^+$ Lin^-) cells, gene expression data in FPKM was obtained from RNA-sequencing data by aligning paired end unstranded 100bp poly-A reads using STAR and quantifying genes using Cufflinks.
(A) Whole gene signature of sAML LSC versus normal aged progenitors showing patterns of significant differential gene expression (FPKM>1, $p<0.05$, absolute L2FC>1).
(B) The gene expression data was submitted for gene set enrichment analysis (GSEA) to determine enriched KEGG pathways in benign versus malignant progenitor cell aging. Venn diagram summarizes the unique and intersecting enriched KEGG pathways (FDR<25% for gene sets with positive normalized enrichment scores) in aged versus young normal progenitors and sAML versus aged progenitors.
(C) Relative expression of *SF3B1* was assessed by qRT-PCR (left panel) in FACS-purified AML versus normal progenitors ($p<0.05$ by unpaired, two-tailed Student's t-test; §=primary sample harboring a point mutation in exon 14 of *SF3B1*). Sanger sequencing (right panel) verified one coding SNV in *SF3B1* in progenitors from AML-41.
(D) sAML-specific splice isoform expression patterns were evaluated in an additional cohort of aged and young progenitors (n=2 per group) and cord blood progenitors (n=3).
(E) Expression profiles of sAML splice isoform signature transcripts that mapped to UCSC identifiers in publicly available TCGA isoform datasets from RNA-Seq studies performed on unsorted AML leukemic cells (n=164 samples). Samples (n=156) clustered into six dominant subgroups (n=9-55 per group) based on sAML-associated transcript expression (log2 TPM+1).

Figure S3 (related to Fig. 2)

A Enrichment plot in MDS v. aged: KEGG spliceosome

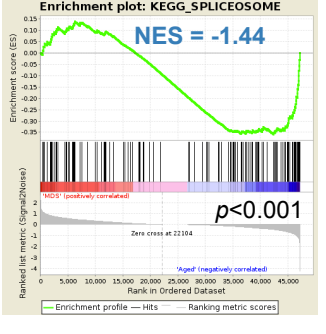

B Enrichment plot in MDS v. aged: sAML LSC-associated transcripts

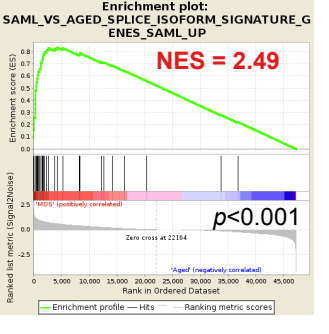

C GSEA: sAML v. MDS

NAME	SIZE	NES	NOM p-val	FDR q-val
KEGG_CYTOKINE_CYTOKINE_RECEPTOR_INTERACTION	256	2.00	<0.001	0.002
AGED_VS_YOUNG_SPLICE_ISOFORM_SIGNATURE_GENES_AGED_UP	55	1.92	<0.001	0.002
KEGG_TOLL_LIKE_RECEPTOR_SIGNALING_PATHWAY	97	1.96	<0.001	0.002
KEGG_FC_GAMMA_R_MEDIATED_PHAGOCYTOSIS	96	1.87	<0.001	0.004
KEGG_SYSTEMIC_LUPUS_ERYTHEMATOSUS	134	1.88	<0.001	0.005
KEGG_ERBB_SIGNALING_PATHWAY	87	1.84	<0.001	0.006
KEGG_COLORECTAL_CANCER	62	1.83	<0.001	0.006
KEGG_FC_EPSILON_RI_SIGNALING_PATHWAY	79	1.82	<0.001	0.007
KEGG_B_CELL_RECEPTOR_SIGNALING_PATHWAY	74	1.81	<0.001	0.007
KEGG_PEROXISOME	78	-1.95	<0.001	0.008

Figure S3. Gene set enrichment analyses of normal, MDS and sAML progenitors.
Gene set enrichment analyses (GSEA) were performed using all KEGG pathways plus custom gene sets including genes associated with the top differentially expressed transcript signatures in aged ("aged up") versus young ("young up") HPC, and sAML ("sAML up") versus aged ("aged up") HPC to identify significant pathways enriched in MDS versus age-matched control HPC, and in sAML versus MDS progenitors.
(A) Enrichment plot showing moderate disruption of spliceosome components in MDS progenitors versus aged HPC.
(B) Enrichment plot showing that genes associated with upregulated splice isoforms in sAML represents the top enriched gene set in MDS progenitors versus aged HPC.
(C) Top gene sets deregulated in sAML versus MDS progenitors are shown (false discovery rate, FDR<1%). NES=normalized enrichment score.

Figure S4 (related to Fig. 4)

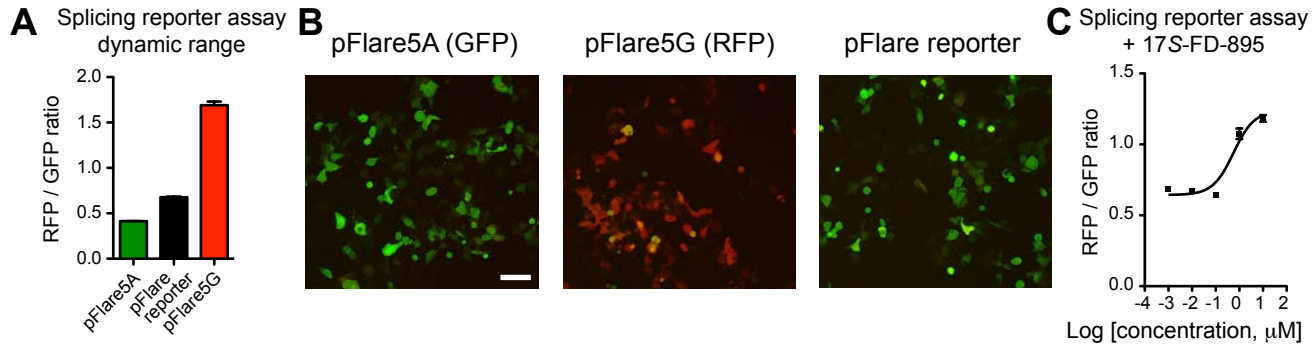

Figure S4. Splicing Reporter Assays in HEK293 Treated with 17*S*-FD-895.

(A) Dynamic range of the splicing reporter assay. HEK293 cells were transfected with GFP (pFlare5A) or RFP (pFlare5G) vector controls(Stoilov et al., 2008), or the pFlare reporter vector (n=2-3 separate wells per condition). Forty-eight hours after transfection, cells were dissociated and analyzed by flow cytometry to determine the transfection efficiency and mean fluorescence intensity (MFI) of transfected cells.

(B) Fluorescent microscopy images of HEK293 cells transfected with pFlare vectors (no treatment). pFlare5A represents the GFP-expressing control, while pFlare5G represents the RFP-expressing control. Cells were imaged 24 h after transfection. Scale bar = 75 μm.

(C) For *in vitro* fluorescence reporter-based validation of splicing attenuation, HEK293 cells were treated with 17*S*-FD-895 at doses from 0.01 – 10 μM starting 24 h after transfection with the pFlare splicing reporter. After 24 hrs of treatment with 17*S*-FD-895, cells were analyzed by flow cytometry and splicing activity was calculated as the ratio of RFP/GFP MFI.

Figure S5 (related to Fig. 5)

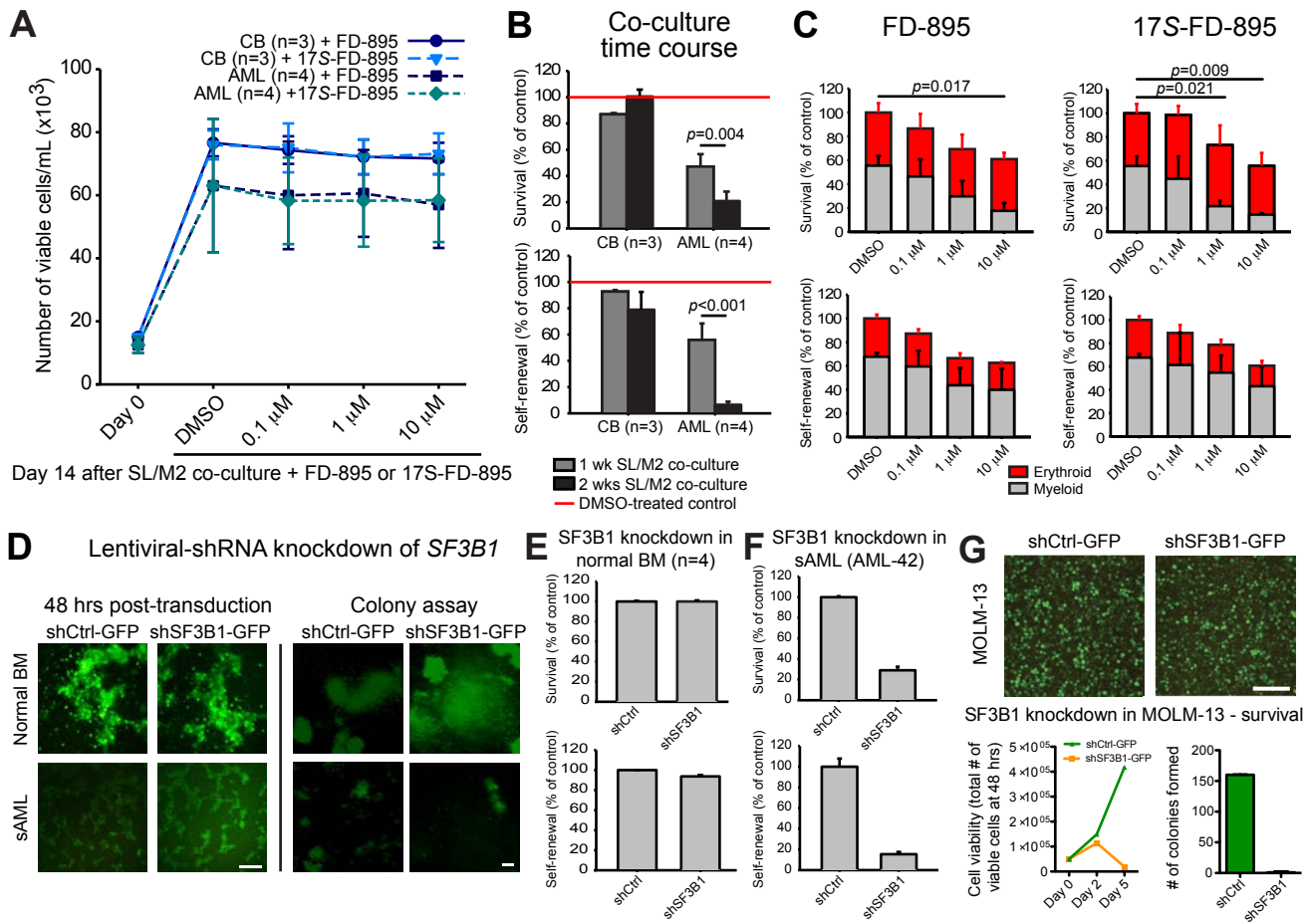

Figure S5. Time Course and Hematopoietic Progenitor Cell Fate Studies in Bone Marrow Stromal Co-Cultures Treated with 17*S*-FD-895.

(A) Viability of CD34-selected normal cord blood (CB, n=3) and AML LSC (n=4) after two weeks of co-culture with SL/M2 bone marrow stroma in the presence of DMSO control, FD-895 or 17*S*-FD-895 (0.1 – 10 μM).

(B) Survival and self-renewal assays for CD34-selected normal cord blood (CB, n=3) and AML LSC (n=4) after one or two weeks of co-culture with SL/M2 bone marrow stroma and treatment with 17*S*-FD-895 (1 μM, $p<0.01$ compared to one week co-cultures by one-way ANOVA).

(C) Hematopoietic progenitor assays showing that FD-895 and 17S-FD-895 reduces myeloid colony formation of normal aged bone marrow samples (n=3), with no effect on erythroid colonies ($p<0.05$ for CFU-GM compared to DMSO-treated controls by one-way ANOVA).

(D-G) Lentiviral-shRNA knockdown of *SF3B1* in aged bone marrow samples, sAML, or MOLM-13 cells. For *in vitro* survival and self-renewal assays, CD34+ cells from primary patient samples or unselected MOLM-13 cells were transduced with lentiviral vectors (shCtrl-GFP or shSF3B1-GFP, MOI=100) and subsequently transferred to MethoCult for replating assays.

(D) Fluorescence microscopy images of lentivirally-transduced normal aged bone marrow (n=4) and sAML (n=1) samples. Scale bar = 200 μm.

(E, F) Survival and self-renewal of normal HSPC (E) and AML LSC (F) in replating assays.

(G) Fluorescence microscopy images of lentivirally-transduced MOLM-13 cells (48 hrs after transduction, upper panels) and overall reduction in cell viability (lower panel, left) 5 days after transduction with shSF3B1 lentivirus (n=2) and cell survival in colony formation assays (lower panel, right). Scale bar = 200 μm.

Figure S6 (related to Fig. 6)

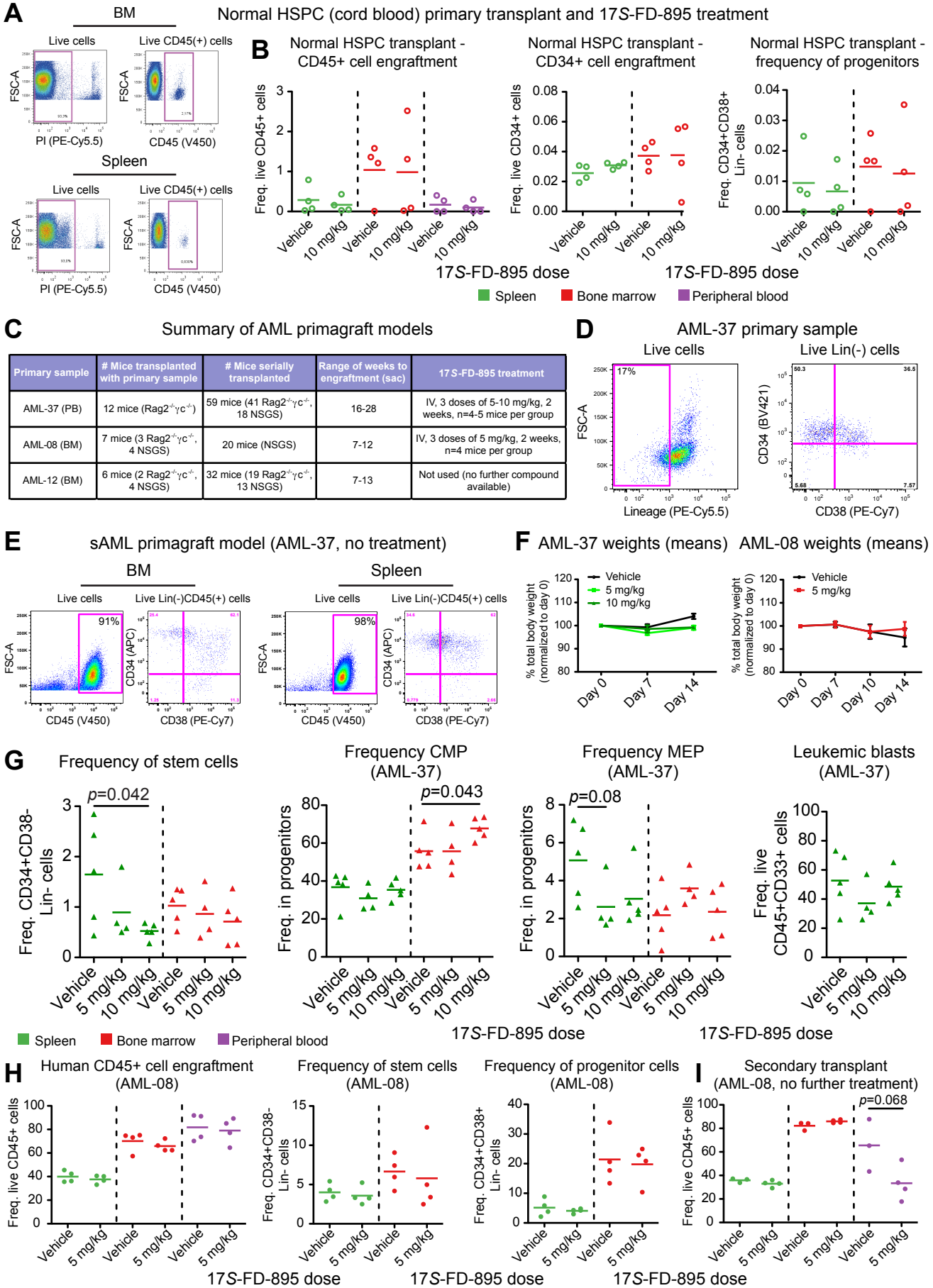

Figure S6. Normal HSPC In Vivo Models, Serially Transplantable AML Primagraft Models, and Human Stem and Progenitor Cell Analyses After *In Vivo* 17*S*-FD-895 Treatment.

(A) Representative FACS plots showing engraftment of normal cord blood-derived hematopoietic cells in immunocompromised mice.

(B) FACS analysis of human total $CD45^+$ cells and hematopoietic stem and progenitor cell engraftment in hematopoietic tissues from mice transplanted with $CD34^+$ cord blood cells followed by treatment with vehicle (DMSO, n=4), 17*S*-FD-895 (10 mg/kg, n=4).

(C) Summary of AML patient samples used to establish AML primagraft models in immunocompromised mice (n=136 mice transplanted). All primary and serial transplantations were performed using 1-2 x 10^5 $CD34^+$ (LSC-enriched) cells.

(D) FACS plots showing live, lineage-negative stem ($CD34^+CD38^-$) and progenitor ($CD34^+CD38^+$) cell populations in AML-37.

(E) Representative FACS plots showing robust engraftment of AML LSC in immunocompromised mice.

(F) Mouse weights over the two-week treatment period in AML primagraft studies.

(G) FACS analysis of human hematopoietic stem ($CD34^+CD38^-Lin^-$), CMP ($CD34^+CD38^+CD123^+CD45RA^-$), MEP ($CD34^+CD38^+CD123^-CD45RA^-$) cell engraftment, and leukemic blast burden ($CD45^+CD33^+$) in hematopoietic tissues of mice transplanted with AML-37 and treated with vehicle (DMSO, n=5) or 17*S*-FD-895 (5 mg/kg, n=4; 10 mg/kg, n=5). All graphs show mean values and statistical analysis by Student's t-test.

(H) FACS analysis of human total $CD45^+$ cells and hematopoietic stem and progenitor cell engraftment in hematopoietic tissues from mice transplanted with AML-08 and treated with vehicle (DMSO, n=5), 17*S*-FD-895 (5 mg/kg, n=4; 10 mg/kg, n=5).

(I) For serial transplantation experiments, CD34-selected cells from AML-08 primagrafts were pooled from the individual hematopoietic tissues from mice in each treatment group (n=4-5 per group) and transplanted intravenously into serial transplant recipients. Human cell engraftment ($CD45^+$) was analyzed by flow cytometry 11 weeks after transplant. All graphs show mean values and statistical analysis by unpaired, two-tailed Student's t-test ($p<0.05$ compared to vehicle-treated controls).

Figure S7 (related to Fig. 7)

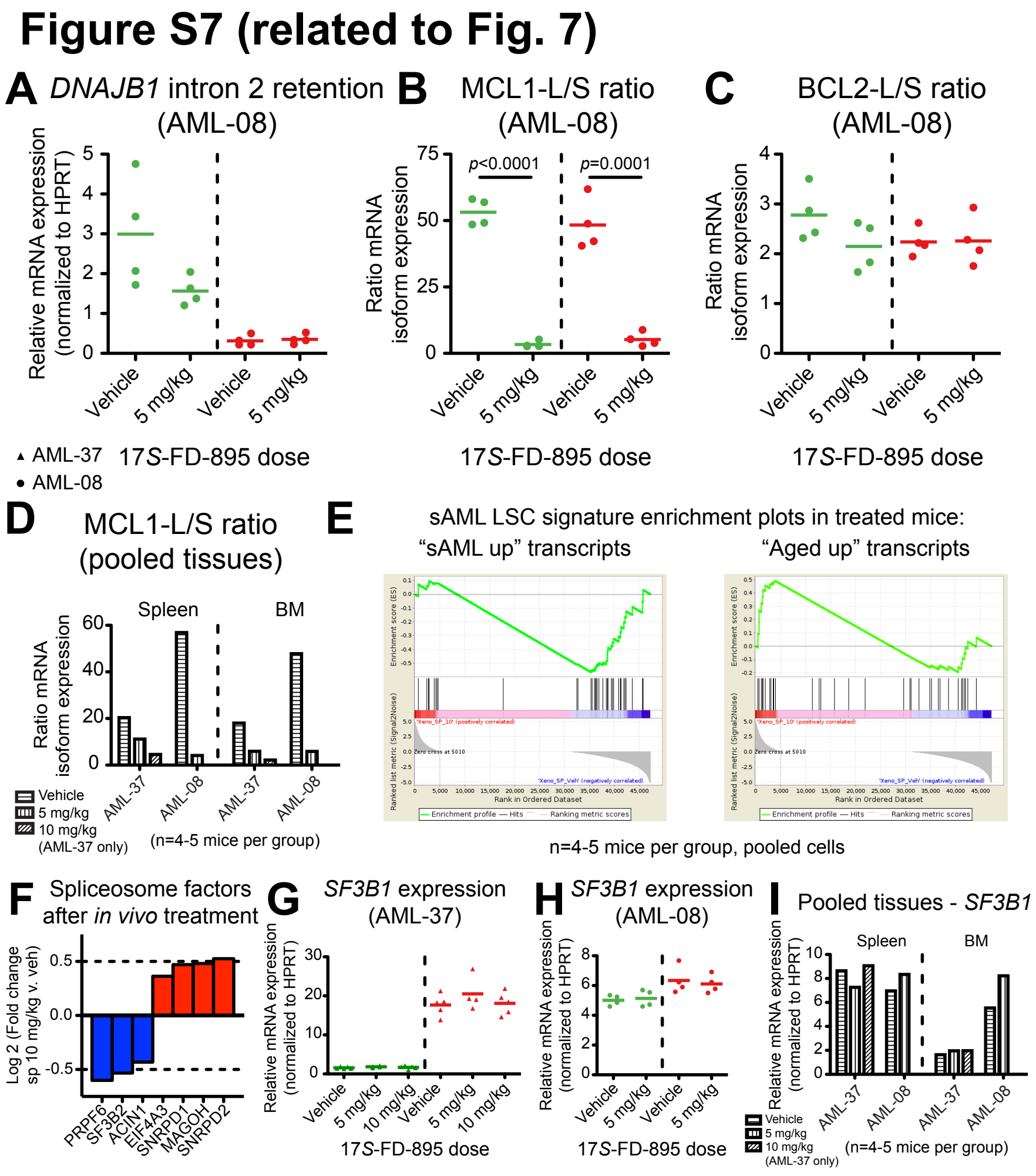

Figure S7. Quantitative RT-PCR Analysis and RT-PCR in AML Primagraft Models After Splicing Modulator Treatment. For qRT-PCR analysis of *in vivo* splicing alterations, single cell suspensions from hematopoietic tissues of 17*S*-FD-895-treated mice were CD34-selected and processed for RNA extraction and cDNA preparation or RNA-Seq analysis.
(A-C) Quantification of DNAJB1 intron 2 retention (A) and MCL1-L/S (B) and BCL2-L/S (C) ratios in $CD34^+$ cells from the spleens of individual AML-08 mice treated with vehicle or 17*S*-FD-895.
(D-F) Aliquots of pooled $CD34^+$ cells prepared for serial transplantation studies were analyzed by qRT-PCR and RNA-Seq.
(D) Reduced MCL1-L/S expression ratios in pooled $CD34^+$ cells from 17*S*-FD-895-treated mice,
(E) GSEA enrichment plot showing genes associated with upregulated splice isoforms in sAML ("sAML up") and downregulated splice isoforms in sAML ("aged up") were depleted and enriched, respectively, in the 10mg/kg 17*S*-FD-895 treated mice compared with vehicle-treated controls. The "aged up" genes represented the third most enriched gene set in the spleens of pooled $CD34^+$ cells from mice that received splicing modulator treatment.
(F) RNA-Seq-based splicing factor gene expression changes in the spleens of treated mice.
(G-I) qRT-PCR analysis of *SF3B1* mRNA expression in 17*S*-FD-895-treated AML primagrafts (individual mice, G, H) or pooled cells used in serial transplantation assays (I).
All graphs show mean values and statistical analysis by unpaired, two-tailed Student's t-test ($p<0.01$ compared to vehicle-treated controls).

SUPPLEMENTAL TABLES

All Supplemental Tables are also available as additional supplemental materials in Excel format.

Table S1 (related to Figure 2). AML and MDS patient samples used for RNA-sequencing, qRT-PCR, functional studies and to establish humanized AML primagraft models.

Sample Code	Gender	Age	Cell Source	Blast %	Diagnosis	Prior Disease	Treatment	Cytogenetics
AML-04	M	76	BM	M=88%, F=95%	AML	AML	None	46,XY,del(7)(q22)[3]/46,XY[6]
*AML-08	F	52	BM	M=37%, F=42.1%	AML	AML	None	46,XX[20]
*AML-12	M	51	BM	M=38%, F=31%	AML	AML	None	46,XY[20]
AML-22	F	60	BM	M=14%, C=7%	AML (NOS)	1st relapse	N/A	N/A
AML-23	M	66	BM	M=50%, C=70%	AML (M0)	1st relapse	N/A	N/A
AML-24	M	70	BM	M=13%, C <5 %	AML	1st relapse	N/A	N/A
AML-25	M	66	BM	M<5%, C=0	AML (M1)	1st relapse	N/A	N/A
AML-26	F	47	BM	M=60.3%, C <1%	AML (NOS)	1st relapse	N/A	N/A
AML-27	F	73	BM	M=0% - relapse quantified by monocytoid cells	AML (M5b)	1st relapse	N/A	N/A
AML-28	M	72	PB	M=41%, C=6%	AML (NOS)	1st relapse	N/A	N/A
AML-29	M	61	PB	M=90%, C=45%	AML (M1)	1st relapse	N/A	N/A
AML-31	M	59	PB	PB=10%	sAML	MDS	None	N/A
*AML-32	M	68	PB	50%	sAML	MDS	None	47,XY,+8[2]/46,XY[18]
*AML-33	F	63	BM	M=21%, F=5.8%	sAML	MDS	None	47,XX+21[14]/46,XX,+mar1[2]/46,XX[4]
*AML-35	M	82	BM	M=12%, F=28.2%	sAML	MDS	None	45,X,-Y[20]
*AML-37	F	72	PB	PB=63%	sAML	MDS	None	46,XX,1,inv(3)(q21q26.2),del(5)(q14q34),der(12)t(1;12)(q21;p11.2),20,+r,+mar1[9]/ 46,sl,der(7)t(7;9)(p13;q13)[4]/46,sl,i(21)(q10)[3]/46,sl, add(2)(q31)[2]/46,sl,add(2)(q33)[2]
*AML-39	F	69	PB	PB=79.8%	sAML	MPD	None	46,XX[10]
*AML-40	F	63	PB	5% CD34+, 19%	sAML	MDS	None	5q-, +8, possible 7q-
*AML-41	M	82	BM	N/A	sAML	MDS (RARS)	Hydroxyurea	N/A
AML-42	M	73	BM	92%	sAML	CMML	None	N/A
AML-43	M	72	PB	14% in BM	sAML-M6	MDS	None	N/A
AML-44	M	74	BM	N/A	sAML	MF	Revlimid	N/A
*MDS-06	F	62	PB	M=<5%, F=14%	MDS/MF	None known	None	5q deletion; JAK2V617F negative
*MDS-07	M	74	PB	M=4.5%, F=1.7-2.3%	MDS/MF	None known	G-CSF	Normal FISH results in bone marrow, JAK2V617F negative
*MDS-10	M	71	BM	M=<1%	MDS	None known	None	Normal FISH results in bone marrow, JAK2V617F negative
*^MDS-12	M	48	PB	F=9%	MDS-RAEB2	Newly diagnosed	None	45~47,X,add(Y)(q11.23),add(4)(q12),der(5;17)(p10;q10),-6,del(7)(q22q34),+8,-18,add(18)(q11.2),-20,-22,+1~3r,+mar1,+2~4mar[cp20]
*^MDS-13	M	48	BM	M=13%, F=4.4%	MDS-RAEB2	Newly diagnosed	None	45~47,X,add(Y)(q11.23),add(4)(q12),der(5;17)(p10;q10),-6,del(7)(q22q34),+8,-18,add(18)(q11.2),-20,-22,+1~3r,+mar1,+2~4mar[cp20]

M = morphology, F = flow (peripheral blood), C = circulating blasts (peripheral blood), BM = bone marrow, PB = peripheral blood, NOS = not otherwise specified, MPD=myeloproliferative disorder, N/A = not available
*Samples used in RNA-seq studies; ^from same sample donor

Table S2 (related to Figures 1 and 2, see supplemental Excel file). Gene set enrichment analyses (GSEA) showing differentially regulated pathways in aging human HSC, HPC, and sAML LSC (FDR<25%).

Table S3 (related to Figures 1-3, see supplemental Excel file). Significantly differentially expressed genes (FPKM>1, p<0.05, absolute L2FC>1) in aged versus young human HSC, aged versus young human HPC, and sAML versus normal aged HPC.

Table S4 (related to Figures 1-3, see supplemental Excel file). Significantly differentially expressed isoforms (FDR<5%) in aged versus young normal HSC (n=4 per group) and a validation cohort of additional normal HSC (#n=3 additional aged samples) analyzed on an updated RNA-seq platform. FPKM values are shown for all isoforms with average FPKM>1 in aged or young HSC, absolute L2FC>1, FDR<5% (q<0.05).
Significantly differentially expressed isoforms (FDR<5%) in aged versus young normal HPC (n=6 per group), including comparative values in normal CB HPC (n=3) and a validation cohort of additional normal adult HPC (#n=2 per group). FPKM values are shown for all isoforms with average FPKM>1 in aged or young HPC, absolute L2FC>1, FDR<5% (q<0.05).
Significantly differentially expressed isoforms (FDR<5%) in sAML LSC (n=7) versus aged normal HPC (n=6), including comparative values in MDS progenitors (n=5, with 4 unique patient samples) and normal CB HPC (n=3). FPKM values are shown for all isoforms with average FPKM>1 in normal or sAML progenitors, absolute L2FC>1, FDR<5% (q<0.05).

Table S5 (related to Experimental Procedures, see supplemental Excel file). Single nucleotide resolution analysis of RNA-Seq data from sAML LSC (n=7) versus normal age-matched HPC (n=6) at known mutated loci in spliceosome genes (*SF3B1, SRSF2, U2AF1, ZRSR2*) that have previously been associated with MDS/sAML.

Movie S1 (related to Figure 4). Time-lapse imaging showing the effects of 17*S*-FD-895 on splicing activity in a dual fluorescence splicing reporter assay. The previously described pFlare alternative splicing reporter vector (Stoilov et al., 2008) was used to visualize *in vitro* splicing modulation by 17*S*-FD-895 in HEK293 cells. Twenty-four hours after transfection, cells were incubated with 10 μM 17*S*-FD-895 and monitored by time-lapse imaging from 1 hr-24 hrs after treatment initiation, to allow sufficient time for translation of RFP. Images were obtained on an Olympus FV10i confocal microscope at 3-minute intervals.

SUPPLEMENTAL EXPERIMENTAL PROCEDURES

Study Design

The overall research objectives of this study were to both discover new splice isoform biomarkers specific to human hematopoietic stem and progenitor cell (HSPC) aging and sAML LSC, and evaluate the potent and stable spliceosome-targeted small molecule compound 17*S*-FD-895 in AML LSC survival and self-renewal assays in pre-clinical models. In controlled laboratory experiments, research samples included primary peripheral blood or bone marrow samples from consenting AML patients (n=22) and age-matched normal control bone marrow samples (n=14) obtained from healthy volunteer individuals undergoing hip replacement therapy for reasons other than leukemia, or normal cord blood (n=6) or young bone marrow (n=8) controls obtained from a commercial source (AllCells, Alameda, CA). For experiments using primary samples, the sample size of each experiment is limited by the availability of rare and valuable samples specific for disease and stage from patients. To discover new splice isoform biomarkers specific to human HSPC aging compared with sAML LSC, primary AML and normal control (age-matched or young) samples were FACS-purified and analyzed by RNA-Seq, and whole transcriptome analyses and hierarchical clustering analyses were utilized to establish unique splice isoform expression signatures. We use a definition of significance as a two-sided alpha level of 0.05 and aim to have power of 0.80. Based on an expected effect size that is twice the standard deviation we can achieve 0.79 power with five samples per arm based on a normal distribution. The goal of each experiment is to get close to five or more samples per arm depending on clinical sample availability and viability. The effect size we are able to detect with this power is variable based on intra-arm sample variability via standard deviation. Consistent with AML genetic heterogeneity, there was some variability in primary patient sample analyses by RNA-Seq and qRT-PCR. When considering sequencing of multiple genes it is assumed that a much larger effect size will be required due to appropriate adjustment for multiple comparisons. For this reason, a false-discovery rate (FDR) correction was applied.

In hypothesis-driven experiments, the splicing modulatory compound 17*S*-FD-895 was tested to determine efficacy in altering splicing activity in cell lines, and to evaluate effects on AML LSC survival and self-renewal capacity in humanized bone marrow stromal co-cultures and in primagraft AML LSC models. Cell culture experiments were performed using 293T and sAML (MOLM-13) cell lines, and SL and M2 bone marrow stromal cell lines. Animal studies were performed using immunocompromised $Rag2^{-/-}\gamma_c^{-/-}$ (Abrahamsson et al., 2009) or NOD/SCID-IL2RG mice (Jackson Laboratory, Bar Harbor, ME) (Wunderlich et al., 2010). Primary AML and normal control samples were used in *in vitro* hematopoietic stem and progenitor assays after lentiviral-*SF3B1* knockdown, or bone marrow stromal co-culture and treatment with splicing modulatory compounds (FD-895 or 17*S*-FD-895) or vehicle control (DMSO). Colony formation potential and self-renewal capacity were assessed by counting colony numbers (survival) after two weeks of growth in semi-solid (methylcellulose) media, and subsequent replating capacity (self-renewal) was assessed after transfer to fresh methylcellulose for an additional two weeks of culture. Three primary AML samples were utilized to establish primagraft models in immunocompromised mice, and mice engrafted with cells from two of these models (AML-37 and AML-08) were treated with 17*S*-FD-895 or vehicle (DMSO) to evaluate changes in AML LSC survival and self-renewal capacity *in vivo*. One primary normal cord blood (CB) sample was used to establish a primagraft model to evaluate 17S-FD-895 effects on normal HSPC survival and self-renewal potential. Data were collected by flow cytometry, qRT-PCR and RNA-Seq analysis of CD34-selected human LSC-enriched cells from engrafted mice.

In *in vivo* experiments, before initiation of treatment, CB or AML-engrafted mice were distributed among treatment groups according to human cell engraftment rates ($CD45^+$ cell frequency) in peripheral blood, and total body weights (average engraftment and body weights for each treatment were equal at the initiation of treatment). Inclusion/exclusion criteria for AML primagrafts were pre-established based on minimum $CD45^+$ cell engraftment rates of 1% in peripheral blood, and endpoints included human stem and progenitor engraftment analyses as

established by previous primagraft experiments (Abrahamsson et al., 2009; Jamieson et al., 2004). All qRT-PCR analyses were performed using two technical replicates for each sample, with the average of the two replicates shown in all graphs. For *in vitro* experiments, the same investigator performed treatments and analyses. For *in vivo* experiments, investigators performing FACS and qRT-PCR analyses were blinded to each animal's treatment status until after all data were collected.

Reagents

Antibodies – For primary sample FACS purification of hematopoietic stem and progenitor cell populations, CD34-selected (Miltenyi) primary samples were stained with a panel of well-validated human-specific antibodies (Abrahamsson et al., 2009; Goff et al., 2013; Jamieson et al., 2004; Jiang et al., 2013) was utilized. Antibodies included human CD34-APC and CD38-PECy7 (BD Biosciences, San Diego, CA) and lineage markers (CD2, CD3, CD4, CD8, CD14, CD19, CD20 and CD56 cocktail, all antibodies PECy5.5 conjugated, from Life Technologies, Carlsbad, CA). For flow cytometric analyses of primagraft models, the same panel of antibodies was used for analysis of spleen and bone marrow-derived cells, with the addition of CD45-V450, CD123-PE (both from BD Biosciences), and CD45RA-FITC (Life Technologies) for further visualization of progenitor cell subpopulations, or CD45-APC (Life Technologies) and CD33-PE (BD Biosciences), for leukemic blast populations. Due to background autofluorescence in blood, for flow cytometric analysis of peripheral blood from treated mice, the CD34 and CD45 antibodies were replaced with alternative antibodies to exclude FITC labeled reagents (CD34-PE, BD Biosciences and CD45-APC, Life Technologies).

RNA and PCR reagents – All RNA samples were prepared after lysis of live cells in RLT buffer (Qiagen, Germantown, MD) followed by RNA extraction using RNEasy kits according to the manufacturer's instructions (Qiagen). cDNA was synthesized using the First-Strand SuperScript III Reverse Transcriptase Supermix (Life Technologies) and qRT-PCR was performed using SYBR GreenER Super Mix (Life Technologies). All primers were synthesized by ValueGene (San Diego, CA).

Cell culture reagents – All media (DMEM, RPMI, IMDM) and supplements (Glutamax, penicillin-streptomycin) used in cell culture were from Corning (Manassas, VA) or Life Technologies. Fetal bovine serum (FBS) was from Gemini Bio-Products (Sacramento, CA). For experiments involving transfection of reporter vector plasmids (Stoilov et al., 2008), HEK293 cells were transiently transfected using Lipofectamine (Life Technologies) according to the manufacturer's instructions.

Sample Processing and Primary HSPC and AML LSC Purification

Peripheral blood or bone marrow samples were processed by Ficoll density centrifugation and viable cells stored in liquid nitrogen. Mononuclear cells from AML patients or normal controls were then further purified by magnetic bead separation of $CD34^+$ cells (MACS; Miltenyi, Bergisch Gladbach, Germany) essentially as previously described (Jiang et al., 2013) for subsequent FACS-purification of hematopoietic stem ($CD34^+CD38^-$ Lin^-) and progenitor ($CD34^+CD38^+$ Lin^-) cell fractions. For the majority of AML patient samples utilized, only very few purified viable HSC were obtained (<5,000 cells on average). Therefore the progenitor fractions were utilized for subsequent RNA-Seq and qRT-PCR analyses as these represent the majority of cells present in LSC-enriched fractions prepared for functional *in vitro* and *in vivo* assays using CD34 selection.

For primary hematopoietic progenitor cell purification, CD34-selected cells were stained with fluorescent antibodies against human CD34 and CD38 (BD Biosciences) and lineage markers (cocktail, all antibodies from Life Technologies) and propidium iodide as previously described(Abrahamsson et al., 2009; Jamieson et al., 2004; Jiang et al., 2013). Following staining, cells were analyzed and sorted using a FACS Aria II (Sanford Consortium Stem Cell Core Facility), and hematopoietic stem ($CD34^+CD38^-$ Lin^-) and progenitor ($CD34^+CD38^+$ Lin^-) populations were isolated. Freshly-sorted cells were collected in lysis buffer (Qiagen) for RNA extraction followed by RNA-Seq (The Scripps Research Institute Next Generation Sequencing Core) on Illumina HiSeq (all discovery sample sets) or NextSeq (xenograft samples and some validation sample sets) platforms, or qRT-PCR analyses as previously described (Jiang et al., 2013).

Nucleic Acid Isolation and PCR (qRT-PCR and RT-PCR)

Primary $CD34^+CD38^+$ Lin^- cells or enriched human $CD34^+$ cells from mouse tissues were isolated using FACS purification or CD34 microbead-selection, and 2-10 x 10^4 cells were harvested in lysis buffer (Qiagen). RNA was purified using RNeasy micro RNA purification kits with a DNase (Qiagen) incubation step to digest any trace genomic DNA present. RNA was stored at -80°C. Immediately prior to reverse transcription of RNA samples, nucleic acid concentrations were quantified on a NanoDrop 2000 spectrophotometer (Thermo Scientific), and purity was considered acceptable if A260/A280 values were >1.8. Samples submitted for RNA-Seq were further subjected

to quality control assessment on an Agilent Bioanalyzer (The Scripps Research Institute Next Generation Sequencing Core). Samples with RNA integrity (RIN) values > 7 were used for RNA-Seq.

For qRT-PCR analysis of relative total mRNA expression levels or splice isoform-specific expression analyses, cDNA was synthesized using 50 ng - 1 μg of template RNA in 20 μL reaction volumes using the First-Strand SuperScript III Reverse Transcriptase Supermix (Life Technologies) followed by incubation with RNase H according to the manufacturer's protocol and as described previously (Abrahamsson et al., 2009; Crews et al., 2015). All cDNA products were stored at -20°C. Splice isoform-specific primers for *PTK2B-202* were designed to bind to unique exon junctions for this transcript, which lacks exon 24. All primers (Supplemental Experimental Procedures Table) were diluted to 10 μM working dilutions in DNase/RNase-free water. qRT-PCR was performed in duplicate using cDNA (1 μL reverse transcription product per reaction) on an iCycler (Bio-Rad, Hercules, CA) using SYBR GreenER Super Mix (Life Technologies) in 25-μL volume reactions containing 0.2 μM of each forward and reverse primer. Cycling conditions were as follows: 50°C for 2 minutes, then 95°C for 8 minutes and 30 seconds, followed by 40 cycles of 95°C for 15 seconds and 60°C for 60 seconds. Melting curve analysis was performed on each plate according to the manufacturer's instructions. For standard qRT-PCR, human HPRT mRNA transcript levels were used to normalize Ct values obtained for each gene, and relative expression levels were calculated using the 2^{-ddCt} method. To ensure validity of results, only Ct values <35 were used in gene expression analyses. All primer sets were tested in a no-template control (NTC) reaction containing only water instead of cDNA, and all gave Ct values >35 in NTC reactions.

Supplemental Experimental Procedures Table. Primers used for qRT-PCR, RT-PCR and direct sequencing analyses

Gene	Primer Set	FW 5'-3'	REV 5'-3'	Reference
Human *HPRT*	Total (qRT-PCR)	TCAGGGATTTGAATCATGTTTGTG	CGATGTCAATAGGACTCCAGATG	Crews et al., 2015
SF3B1 (ex14)	Total (qRT-PCR)	AGCTTTTGCTGTTGTAGCCTCTG	GCTTGCCAGGACTTCTTGCT	Jeromin et al., 2013
BCL2-L	Isoform-specific (qRT-PCR)	ATGTGTGTGGAGAGCGTCAA	TTCAGAGACAGCCAGGAGAAA	Goff et al., 2013
BCL2-S	Isoform-specific (qRT-PCR)	ATGTGTGTGGAGAGCGTCAA	CTCAGCCCAGACTCACATCA	Goff et al., 2013
MCL1-L	Isoform-specific (qRT-PCR)	AGACCTTACGACGGGTTGG	AATCCTGCCCCAGTTTGTTA	Goff et al., 2013
MCL1-S	Isoform-specific (qRT-PCR)	GAGGAGGACGAGTTGTACCG	ACTCCACAAACCCATCCTTG	Goff et al., 2013
BCLX-L	Isoform-specific (qRT-PCR)	CATGGCAGCAGTAAAGCAAG	GAAGGAGAAAAAGGCCACAA	Goff et al., 2013
PTK2B-202	Isoform-specific (qRT-PCR)	CTGCAGTTCCAGGAGGAG	CTGTGAACTCCAGGTAGCC	New
DNAJB1 (in2)	Intronic (qRT-PCR)	GGCCTGATGGGTCTTATCTATGG	TTAGATGGAAGCTGGCTCAAGAG	Kotake et al., 2007
SF3B1 (ex10-17)	Sequencing (PCR)	TGACCAGCCATCTGGAAATC	CACCATCTGTCCCACAACAC	Jeromin et al., 2013
DNAJB1	RT-PCR	GAACCAAAATCACTTTCCCCAAGGAAGG	AATGAGGTCCCCACGTTTCTCGGGTGT	Kotake et al., 2007
MCL1	RT-PCR	CTCGGTACCTTCGGGAGCAGGC	CCAGCAGCACATTCCTGATGCC	Kashyap et al., 2015

Whole Transcriptome Sequencing and Determination of Gene and Splice Isoform Expression Values

Gene and isoform expression data in FPKM was obtained from RNA-sequencing data (sequencing performed at The Scripps Research Institute Next Generation Sequencing Core, San Diego, CA) for young (average 66M input reads per HPC sample) and aged (average 73M reads per HPC sample) normal samples, and sAML LSC (average 73M reads per sample) by aligning paired end unstranded 100bp poly-A reads to the human reference genome (GRCh37/hg19) using STAR (Dobin et al., 2013). Transcripts were quantified using Cufflinks to generate FPKM values (Trapnell et al., 2010), and average log2 fold change (L2FC) and *p* values for genes and isoforms were obtained as previously described (Kirschner et al., 2015; Kumar et al., 2014)(Tables S3 and S4). All gene and transcript names correspond to the identifiers used in Ensembl GRCh37.

Xenograft sequencing data of 2x150 bp paired end reads were trimmed using cutadapt 1.8.1, aligned using STAR 2.5.0b against the GRCh37 reference FASTA with the Ensembl GRCh37.75 GTF as a splice junction source. Strandedness was inferred using infer_experiment.py from the RSeQC package (Wang et al., 2012). Then, transcripts were quantified using Cufflinks v2.2.1 (Trapnell et al., 2010) against the Ensembl GRCh37.75 GTF reference with bias correction against the GRCh37 reference FASTA. This yielded Cufflinks FPKM values. Isoforms sharing gene names were summed to yield gene FPKMs. FPKM values were transformed to generate

log2(FPKM+1) for all transcripts in the sAML isoform signature (Table S4), comparing vehicle versus 10 mg/kg treatment groups for spleen and bone marrow. Then, a heatmap was generated using all transcripts showing a L2FC>0.5 in both tissues, occurring in the opposite direction of the L2FC transcript expression values in sAML versus normal age-matched controls (i.e. L2FC>1 in sAML, L2FC<-0.5 in 10 mg/kg-treated spleen and bone marrow).

RNA-Seq Based Gene Set Enrichment, Gene Ontology, Network Analyses, Generation of Splice Isoform Signatures, and Principal Components Analysis

Gene expression data in FPKM was submitted to GSEA to determine significant KEGG pathways, and enrichment plots describing ranked gene expression in those pathways. Additional analyses were performed using custom gene sets including genes associated with the top differentially expressed transcript signatures in aged ("aged up") versus young ("young up") HPC and sAML ("sAML up") versus aged ("aged up") HPC (Table S4). We acknowledge our use of the gene set enrichment analysis, GSEA software, and Molecular Signature Database (MSigDB, http://www.broad.mit.edu/gsea/). Network analyses were performed on top differentially expressed isoforms by inputting their corresponding gene identifier names into Cytoscape's Reactome FI plugin. All significantly differentially expressed genes in normal aged versus young HSC and HPC, or aged versus sAML samples, were probed for human transcription factors (Zhang et al., 2012), and commonly DE transcription factors were identified.

After FDR correction (FDR<5%, as described in main Experimental Procedures), to identify the top differentially expressed splice isoforms in aged versus young HSC, aged versus young HPC, and sAML LSC versus normal age-matched HPC, a calculation was performed to generate a composite value reflecting both the significance of the difference between groups (*p* value) and the magnitude of the difference (fold change). Graphical representations of *p* values versus fold change for large expression datasets are often visualized as volcano plots, however most selection criteria for identifying the top differentially expressed factors rely on dual cutoffs such as $p<0.05$ or L2FC>1, or manual selection of transcripts which relies on subjective criteria (as described for microarray data visualized by volcano plot on the NCI Genomics and Bioinformatics group website at http://discover.nci.nih.gov/microarrayAnalysis/Statistical.Tests.jsp). To alleviate any manual bias of selecting "top differentially expressed transcripts", we generated volcano plots for all transcripts with an average FPKM>1 in one condition of the comparison, and applied *p*-value (<0.05) and L2FC (>1) cutoffs. Then, the remaining transcripts were ranked by quantifying the relative Cartesian distance from the origin on a volcano plot, where the average L2FC of each transcript is displayed on the x-axis and the –log10(*p* value) on the y-axis. The formula applied for calculating the composite values was: $\sqrt{((L2FC^2)+(-\log10(p\ value))^2)}$. We then selected the top 75 transcripts for the splice isoform signatures and associated heat maps using the highest-ranking (high to low values) transcripts according to this composite value, which we termed the "Volcano Vector Value". For isoform analyses, these values produced a list of transcripts that was similar to the top transcripts ranked by FDR, but included additional transcripts displaying a large magnitude of fold change. The complete sets of transcripts that passed *p*-value, FDR, and L2FC cutoffs are provided in Tables S3 and S4, to allow for analysis of all transcripts that were differentially expressed in compared groups.

Generation of heatmaps and clustering analyses were performed using GENE-E (http://www.broadinstitute.org/cancer/software/GENE-E/). Gene and isoform expression heat maps were generated using GENE-E default settings and gene expression data for transcripts selected from the list of significantly differentially expressed genes/isoforms with $p< 0.05$ absolute L2FC>1. For whole gene analyses, log2 (FPKM+1) values for features that passed specified p value, Q-value (FDR<5%), and log 2 fold change cutoffs were clustered on heatmaps using the GENE-E default hierarchical clustering method and one minus pearson correlation distance metric.

For principal components analysis (PCA), FPKM values for the top 75 aged vs young HPC signature isoforms in aged and young HPC and sAML, AML, and MDS progenitor samples were annotated and transformed using the expression log2 (FPKM+1). The transformed values were submitted to the R function prcomp and visualized using ggbiplot (https://github.com/vqv/ggbiplot).

Analysis of TCGA AML Datasets

Survival data and RSEM gene and transcript quantifications were downloaded from TCGA for all AML (TCGA Disease Code LAML) samples for which this data was available. Top differentially expressed sAML LSC splice isoforms (Figure 2D) were identified, then mapped from Ensembl transcript names to UCSC known transcript IDs using the MySQL interface to UCSC knownGene tables. Of the 75 transcripts in the sAML splice isoform signature, 28 corresponded to known transcripts in the UCSC database (with some of these having two UCSC identifiers that

were associated with a single ensembl transcript). The UCSC-mapped sAML LSC transcript IDs were then used to retrieve the "scaled_estimate" value for that transcript and sample, multiplied by 10^6 to yield TPM quantifications. Transcripts with a mean TPM of at least 1 were selected. These were then transformed using log2(TPM+1) to yield logTPM quantifications for clustering in a heatmap using GENE-E. Six Groups were identified manually from the GENE-E clustering by selecting entire dendrogram branches, and these were used to segment the survival data into different curves, visualized using Prism. For the purposes of the survival data, the days to the last known checkup were used as the study dropout date for the patient in lieu of the patient days to death, while living patients were listed as dropping out at the study's end. For *PTK2B* transcript analysis, expression values (TPM) of the PTK2B transcript uc003xfp.1 (mapped to ensembl transcript *PTK2B-001,* GRCh37) in all AML patient samples were ranked from high to low expression. The patient samples corresponding to the upper and lower quartiles of expression were compared for overall survival. The results shown here are in part based upon data from primary AML patient samples generated by the TCGA Research Network: http://cancergenome.nih.gov/ (TCGA 2013).

Mutational Analysis of *SF3B1* and Other Spliceosome Genes

RNA-Seq reads were aligned with the genomic coordinates of known mutations in *SF3B1*, *U2AF1*, *SRSF2* and *ZRSF2* to assess potential somatic mutations in these splicing factor genes that are highly specific for diagnosis of sAML (Lindsley et al., 2015). For RNA-Seq reads from sAML and normal bone marrow progenitors, 100bp reads were obtained. These were cleaned of adapters and primers using cutadapt, then aligned using STAR. REDItools (Picardi and Pesole, 2013) was used to identify putative somatic mutations at loci previously described in MDS or AML samples (Lindsley et al., 2015; Yoshida et al., 2011). One out of seven sAML patient samples in the RNA-Seq dataset harbored a single G>C mutation in exon 14 of *SF3B1* (538 G reads versus 520 C reads), corresponding to an aa change of K666N in *SF3B1*. For validation by PCR and targeted Sanger sequencing analysis of *SF3B1*, 1 μL of first-strand cDNA templates was prepared for PCR in 25-μL reaction volumes using the high-fidelity KOD Hot Start DNA Polymerase kit according to the manufacturer's instructions (EMD Millipore, Temecula, CA). PCR primers for sequencing *SF3B1* in cDNA were located in exon 10 (forward, FW) and exon 17 (reverse, REV, Supplemental Experimental Procedures Table) (Jeromin et al., 2013). PCR cycling conditions were as follows: 95°C for 2 minutes, followed by 35 cycles of 95°C for 20 seconds, 62°C for 10 seconds and 70°C for 10 seconds, with a final extension step of 70°C for 30 seconds. Amplicons of the predicted size were verified for each outer primer set by DNA gel electrophoresis using 10-20 μL of the completed reaction mixture separated on 2% agarose gels containing ethidium bromide and visualized under UV light. Then, 15 μL of each reaction was processed within 24 hrs for PCR purification, and sequencing was performed on ABI 3730xl DNA Sequencers (Eton Bioscience, San Diego, CA). Sanger sequencing was carried out using two primers, a FW and REV primer each localized to exon 14 (Supplemental Experimental Procedures Table). Sequence chromatograms were analyzed using 4Peaks (by A. Griekspoor and Tom Groothuis, www.nucleobytes.com).

Splicing Reporter Assay and *In Vitro* Splicing Analyses

For evaluation of *in vitro* splicing activity using a two-color fluorescent splicing reporter system (Stoilov et al., 2008), HEK293T cells (mycoplasma-free authenticated cell lines obtained from ATCC) were grown in complete media (DMEM + 10% FBS) and transfected with a series of fluorescent protein-expressing plasmids. Vector controls include pFlare5A, which expresses solely GFP, and pFlare5G, which expresses maximal RFP. The pFlare reporter contains microtubule-associated protein tau (MAPT) exon 10 as an indicator of alternative splicing. Under physiological conditions, the pFlare conditional reporter vector allows in-frame expression of GFP but not RFP. In the presence of splicing inhibitors, exon skipping favors production of RFP over GFP. Twenty-four hours after transfection with the three plasmids in separate wells of a 24-well plate, 17*S*-FD-895 or equivalently diluted DMSO vehicle controls (<1%) were added to the media for an additional 24 hrs, to allow sufficient time for translation of the alternatively spliced transcripts driving expression of RFP or GFP protein products. Fluorescence was evaluated on a Leica fluorescent microscope (Sanford Consortium Stem Cell Core facility) and then analyzed by flow cytometry on a Miltenyi MACSQuant to assess transfection efficiency (ranging from over 70% at 24 hrs after transfection to approximately 20% at 48 hrs after transfection) and mean fluorescence intensity (MFI) of RFP and GFP in positive cells. In HEK293 cells transiently transfected with control GFP or RFP vectors, or the pFlare splicing reporter vector, the dynamic range of the assay as measured by MFI of GFP and RFP 48 hours after transfection ranged from 0.41-1.69 for RFP/GFP ratios (Figure S4A). For time-lapse imaging, splicing reporter-transfected cells were transferred to glass-bottom 35-mm dishes and treated with 1-10 μM of 17*S*-FD-895, followed by sequential imaging on an Olympus FV10i confocal microscope equipped with a 5 % CO_2 cell culture incubation chamber (Tokai Hit, Japan) for up to 24 hrs.

For evaluation of *in vitro* splicing activity of endogenous transcripts in HEK293, KG1a, or a sAML cell line, MOLM-13 (mycoplasma-free and cytogenetically-authenticated cell lines obtained from ATCC or DMSZ), cells were plated in complete media (DMEM containing 10% FBS for HEK293, IMDM containing 10-20% FBS for KG1a, and RPMI containing 20% FBS for MOLM-13). The next day, FD-895, 17*S*-FD-895 or DMSO vehicle controls were added at doses ranging from 0.01 – 10 μM for 4 hrs of treatment. For time course experiments in MOLM-13 sAML cells, 17*S*-FD-895 was added to the media at a dose of 0.1 or 1 μM, for 30 mins – 24 hrs of culture. Cells were lysed in RLT buffer (Qiagen) and processed for RNA extraction and subsequent PCR analyses using primers specific for *DNAJB1* or *MCL1* (Supplemental Experimental Procedures Table). For all experiments in cell lines, cells obtained from the vendors were frozen down in bulk at low passage numbers and used within 20 passages to minimize risk of cell line misidentification or acquisition of additional chromosomal abnormalities.

For genetic *SF3B1* down-modulation studies, an additional set of normal (n=4) and sAML (n=8) samples were CD34-selected and then cultured for 24 hrs in Stempro media containing human cytokines, as previously described (Jiang et al., 2013). Cells were transduced with lentiviral vectors (multiplicity of infection = 100) expressing GFP and an shRNA targeting human *SF3B1* or a non-targeting control (Genecopoeia, Rockville, MD). In parallel, MOLM-13 cells were transduced and cultured in complete media. Cell viability was assessed by trypan blue exclusion after 48 hrs of treatment, and fluorescent images were acquired immediately prior to transferring cells to methylcellulose for colony and replating assays. While the viability of the majority of AML samples (7/8) was low following lentiviral transduction with either vector control or shSF3B1, one sAML sample was sufficiently viable after lentiviral transduction to permit colony and replating assays, and showed a reduction in colony survival and self-renewal.

Bone Marrow Stromal Cell Maintenance for Co-Culture Assays

Mouse bone marrow stromal cell lines (SL and M2 mycoplasma-free authenticated cells obtained from ATCC) expressing human interleukin-3 (IL-3), stem cell factor (SCF) and granulocyte-colony stimulating factor (G-CSF), which support erythroid and myeloid cell expansion and differentiation (Hogge et al., 1996), were maintained under standard culture conditions, as previously described(Goff et al., 2013). Briefly, SL cells were grown in complete medium containing DMEM (Corning), 10% FBS, 1% Glutamax, and 1% penicillin-streptomycin (Life Technologies), while M2 cells were grown in complete medium containing RPMI, 10% FBS, 1% Glutamax, and 1% penicillin-streptomycin (all from Life Technologies). Every four passages, cells were selected by addition of G418 and hygromycin to the culture media for one passage (3-4 days), to maintain human cytokine expression. All cell lines were maintained in T-25 or T-75 culture flasks and were passaged at dilutions of 1:5-1:10 every 2-4 days. Low passage aliquots of cells were thawed every two months to ensure consistency of experiments.

Primagraft Models and Engraftment Analyses

All animal studies were performed in accordance with UCSD and NIH-equivalent ethical guidelines and were approved by the Institutional Animal Care and Use Committee (IACUC protocol #S06015). For all *in vivo* experiments, animals of both genders were utilized. For all transplantations into $Rag2^{-/-}\gamma_c^{-/-}$ animals, neonatal mice were transplanted with human cells intrahepatically as previously described (Abrahamsson et al., 2009, Jiang et al., 2013), and for all transplantations into NSGS animals, which constitutively express human stem cell supportive cytokines SCF, GM-CSF and IL-3 (Wunderlich et al., 2010), sublethally irradiated (300 Rad) adult (6-8 weeks old) mice were transplanted intravenously with 1-2 x 10^5 $CD34^+$ human cells. Mice transplanted with 1-2 x 10^5 $CD34^+$ AML LSC-enriched fractions or no-transplant controls were screened for human hematopoietic cell engraftment ($CD45^+$ cells) in peripheral blood by FACS starting at 7-10 weeks post transplant. At 7-28 weeks post-transplant (7-36 weeks old), mice were euthanized, and peripheral blood and single cell suspensions of hematopoietic organs were analyzed for human cell engraftment by FACS. Total cell suspensions from bone marrow and spleen were either transplanted immediately or CD34-selected for transplant into secondary recipient mice (1-2 x 10^5 cells per animal) to expand the cells *in vivo*. Both mouse strains were found to support serial transplantation of all three patient samples, however for subsequent experiments, AML-37 was maintained in $Rag2^{-/-}\gamma_c^{-/-}$ mice and AML-08 was maintained in NSGS mice. Secondary recipient mice were euthanized after 8-23 weeks, and cell suspensions from bone marrow and spleen were CD34-selected for transplant into tertiary recipients for 17*S*-FD-895 treatment. For qRT-PCR analysis of *in vivo* splicing alterations, single cell suspensions from hematopoietic tissues of 17*S*-FD-895-treated mice were CD34-selected and processed for RNA extraction and cDNA preparation. As a normal HSPC in *vivo* control, 1 x 10^5 $CD34^+$ cells from a mixed donor CB (AllCells, Alameda, CA) were injected intrahepatically into neonatal $Rag2^{-/-}\gamma_c^{-/-}$ mice. Transplanted mice and no-transplant controls were screened for human $CD45^+$ cells engraftment in peripheral blood by FACS starting at 5 weeks post-transplant. Treatment was initiated at 8 weeks

post-transplant, and at 10 weeks post-transplant, mice were euthanized, and peripheral blood and single cell suspensions of hematopoietic organs were analyzed for human cell engraftment by FACS.

***In Vivo* 17*S*-FD-895 Treatment, Tissue Analysis and Serial Transplantation**

The 17*S*-FD-895 dosing regimen was selected as the maximum number of doses possible for the treatment of normal and AML primagraft experimental groups with the amount of synthesized compound that was available, and is consistent with weekly IV dosing regimens used in clinical trials of less stable spliceosome inhibitory compounds in patients with solid tumors (Hong et al., 2014). For *in vivo* treatments, a 10 mg/mL stock solution of 17*S*-FD-895 solubilized in DMSO was used. Vehicle control for AML-08 was 15% DMSO in PBS, for AML-37 and CB 20% DMSO in PBS was used. Animals were euthanized within two hours after delivery of the final dose of 17*S*-FD-895, and peripheral blood, spleens and bone marrows were collected for analysis of total human cell and stem and progenitor cell engraftment, and for RNA extraction for splice isoform-specific qRT-PCR.

Flow cytometric analysis was performed on single cell suspensions from each hematopoietic tissue essentially as for primary patient samples, and frequencies of total live human $CD45^+$ cells, $CD45^+CD34^+CD38^-$ Lin^- (stem) cells, $CD45^+CD34^+CD38^+$ Lin^- (progenitor) cells, and CD45+/CD33+ (leukemic blasts) were determined in each tissue. Analysis of progenitor cell subpopulations was performed for AML-37, with GMP identified as $CD123^+CD45RA^+$, CMP as $CD123^+CD45RA^-$ and megakaryocyte-erythroid progenitors (MEP) as $CD123^+CD45RA^-$. For AML-37 treatment, one additional transplanted mouse was treated with vehicle control (total n=6), however this animal was excluded from FACS and qRT-PCR analyses because of development of a femoral mass not typical of AML primagraft models, but suggestive of an infection occurring in the context of the immunocompromised status of the mouse.

For preparation of RNA from human LSC-enriched populations, single cell suspensions from spleen and bone marrow were CD34 double-selected (over two LS selection columns, Miltenyi) and 1-2 x 10^5 cells were collected in lysis buffer or pooled according to treatment group for serial transplantation assays. For serial transplantation of LSC-enriched fractions from treated mice, cells from individual mice were pooled according to treatment group for each hematopoietic tissue, and 2 x 10^5 cells were transplanted intravenously into adult (6-8 weeks old) NSGS mice.

Statistical Analyses

For RNA-seq based comparisons between groups, average log2 fold change (L2FC) and *p* values for genes and isoforms were obtained as previously described (Jiang et al., 2013; Kirschner et al., 2015). Because raw FPKM values are not normally distributed, *p* values were calculated following log2 transformation of the FPKM values (plus 1 to allow log2 transformation of zero values). Quantitative RT-PCR data were measured as a continuous outcome and each group was assessed for distribution and variance. For normally distributed data, unpaired two-tailed Student's t-tests were applied to determine differences in mRNA expression, and values were expressed as individual data points or means (± SEM) from a minimum of two independent experiments. For AML LSC survival and self-renewal assays, differences among groups were assessed using one-way ANOVA with values expressed as means ± SD (for *in vitro* hematopoietic progenitor assays where comparisons were made among multiple sample types and treatment groups), or Student's t-test with values expressed as means ± SEM (for *in vitro* splicing reporter assays) or as means of individual data points representing biological replicates (for *in vivo* engraftment and qRT-PCR analyses). All experiments were performed on blind-coded samples. All statistical analyses were performed using Microsoft Excel, SigmaPlot, or GraphPad Prism (San Diego, CA).

SUPPLEMENTAL REFERENCES

Cancer Genome Atlas Research, N. (2013). Genomic and epigenomic landscapes of adult de novo acute myeloid leukemia. N Engl J Med *368*, 2059-2074.

Dobin, A., Davis, C. A., Schlesinger, F., Drenkow, J., Zaleski, C., Jha, S., Batut, P., Chaisson, M., and Gingeras, T. R. (2013). STAR: ultrafast universal RNA-seq aligner. Bioinformatics *29*, 15-21.

Hogge, D. E., Lansdorp, P. M., Reid, D., Gerhard, B., and Eaves, C. J. (1996). Enhanced detection, maintenance, and differentiation of primitive human hematopoietic cells in cultures containing murine fibroblasts engineered to produce human steel factor, interleukin-3, and granulocyte colony-stimulating factor. Blood *88*, 3765-3773.

Jeromin, S., Haferlach, T., Grossmann, V., Alpermann, T., Kowarsch, A., Haferlach, C., Kern, W., and Schnittger, S. (2013). High frequencies of SF3B1 and JAK2 mutations in refractory anemia with ring sideroblasts associated with marked thrombocytosis strengthen the assignment to the category of myelodysplastic/myeloproliferative neoplasms. Haematologica *98*, e15-17.

Kirschner, A. N., Wang, J., van der Meer, R., Anderson, P. D., Franco-Coronel, O. E., Kushner, M. H., Everett, J. H., Hameed, O., Keeton, E. K., Ahdesmaki, M.*, et al.* (2015). PIM kinase inhibitor AZD1208 for treatment of MYC-driven prostate cancer. J Natl Cancer Inst *107*.

Kumar, R. M., Cahan, P., Shalek, A. K., Satija, R., DaleyKeyser, A. J., Li, H., Zhang, J., Pardee, K., Gennert, D., Trombetta, J. J.*, et al.* (2014). Deconstructing transcriptional heterogeneity in pluripotent stem cells. Nature *516*, 56-61.

Picardi, E., and Pesole, G. (2013). REDItools: high-throughput RNA editing detection made easy. Bioinformatics *29*, 1813-1814.

Trapnell, C., Williams, B. A., Pertea, G., Mortazavi, A., Kwan, G., van Baren, M. J., Salzberg, S. L., Wold, B. J., and Pachter, L. (2010). Transcript assembly and quantification by RNA-Seq reveals unannotated transcripts and isoform switching during cell differentiation. Nat Biotechnol *28*, 511-515.

Wang, L., Wang, S., and Li, W. (2012). RSeQC: quality control of RNA-seq experiments. Bioinformatics *28*, 2184-2185.

Wunderlich, M., Chou, F. S., Link, K. A., Mizukawa, B., Perry, R. L., Carroll, M., and Mulloy, J. C. (2010). AML xenograft efficiency is significantly improved in NOD/SCID-IL2RG mice constitutively expressing human SCF, GM-CSF and IL-3. Leukemia *24*, 1785-1788.

Zhang, H.M., Chen, H., Liu, W., Liu, H., Gong, J., Wang, H., and Guo, A.Y. (2012). AnimalTFDB: a comprehensive animal transcription factor database. Nucleic Acids Res *40*, D144-149.